Two-dimensional AXUV-based radiated power density diagnostics on NSTX-U

Citation: Faust, I., et al. "Two-Dimensional AXUV-Based Radiated Power Density Diagnostics on NSTX-U." Review of Scientific Instruments, vol. 85, no. 11, Nov. 2014, p. 11D856.

As Published: http://dx.doi.org/10.1063/1.4890254

Publisher: AIP Publishing

Persistent URL: http://hdl.handle.net/1721.1/113230

Version: Author's final manuscript: final author's manuscript post peer review, without publisher's formatting or copy editing

Two-dimensional AXUV-based radiated power density diagnostics on NSTX-U[a)]

I.Faust[1], L. Delgado-Aparicio[2], R. E. Bell[2], K. Tritz[3], A. Diallo[2], S. P. Gerhardt[2], B. LeBlanc[2], T. A. Kozub[2], R. R. Parker[1], B. C. Stratton[2]
[1] *MIT - Plasma Science and Fusion Center, Cambridge, MA, 02139, USA*
[2] *Princeton Plasma Physics Laboratory, Princeton, NJ, 08540, USA*
[3] *The Johns Hopkins University, Baltimore, MD, 21209, USA*

(Dated: 25 June 2014)

A new set of radiated-power-density diagnostics for the NSTX-U tokamak have been designed to measure the two-dimensional poloidal structure of the total photon emissivity profile in order to perform power balance, impurity transport and MHD studies. Multiple AXUV-diode based pinhole cameras will be installed in the same toroidal angle at various poloidal locations. The local emissivity will be obtained from several types of tomographic reconstructions. The layout and response expected for the new radially viewing poloidal arrays will be shown for different impurity concentrations to characterize the diagnostic sensitivity. The radiated power profile inverted from the array data will also be used for estimates of power losses during transitions from various divertor configurations in NSTX-U. The effect of in-out and top/bottom asymmetries in the core radiation from high-Z impurities will be addressed.

I. INTRODUCTION

Measurements of total radiated power (P_{rad}) are important for determining global power balance, diagnosing magnetohydrodynamic (MHD) behavior and understanding impurity dynamics in tokamak plasmas. Characterizing the nature of this emission is of utmost importance for the NSTX-U tokamak, requiring the use of specially designed bolometer cameras. A new, 2-dimensional set of pinhole cameras were developed to tomographically reconstruct the radiated power on a single poloidal plane. The system consists of three cameras utilizing photodiodes to image the plasma from separate positions.

It is important to understand the systematic errors from converting measured chord brightnesses to the tomographic poloidal emissivity profile. This underlies the validity and sensitivity of the reconstruction to changes in the camera measurements. The highly shaped nature of NSTX-U plasmas requires validation of inversion methods. Testing tomographic methods on model emissivity profiles provide *a priori* measure of the sensitivity expected on the implemented NSTX-U diagnostic.

II. DIAGNOSTIC OVERVIEW

The wide spectral width necessary for bolometers (.1 nm−1000 nm) requires the use of pinhole-based optics. Pinhole cameras have been used extensively for radiometric measurement on tokamaks, both for bolometry and soft X-ray tomography using linear diode arrays[1]. Multiple measurements along a common axis are used to measure the meridonal plane in a fan-beam geometry. These images are used in tandem with other measurements or symmetries to reconstruct the tokamak plasma. A new set of 3 pinhole cameras based on these principles have been designed to resolve of the characteristics of the total photonic emissivity of expected NSTX-U plasmas on a single poloidal plane.

Each camera is designed utilizing one AXUV20 diode array composed of 20 vacuum-ultraviolet measuring sil-

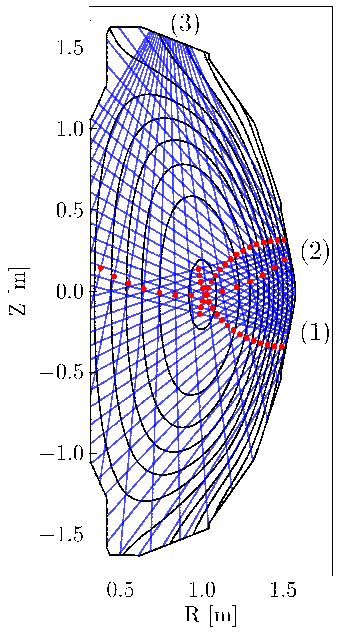

FIG. 1. Chord geometry and plasma equilibrium for synthetic discharge, point of chord tangency to plasma center plotted in red.

[a)] *Contributed paper published as part of the Proceedings of the 20th Topical Conference on High-Temperature Plasma Diagnostics, Atlanta, Georgia, June, 2014.

icon diodes. The diodes provide fast time response, robustness in tokamak environments and wide spectral sensitivity. Unlike an ideal bolometer, the spectral sensitivity of the diode array is variable versus photon energy. For the tested emissivities it is assumed that all emission comes from the region where sensitivity $R \sim .275$ A/W, which is typical of high temperature regions.

The camera placements were chosen to determine profiles of low angular order ($m < 2$) structure, with optimization toward specific Fourier harmonic components associated with impurity asymmetries and MHD modes. The first and second cameras are placed on the low-field side (LFS) above and below the midplane viewing horizontally at downward and upward angles respectively. The offset from the midplane improves the characterization of in-out asymmetries expected in NSTX-U discharges (i.e. improved $\cos\theta$ resolution). However, the strong shaping typical to ST plasmas limited the camera vertical offsets, insuring the reconstruction of the plasma elongation ($\cos 2\theta$ component). The third camera views vertically from the top of NSTX-U into the center stack and lower divertor. Together the three cameras give accurate resolution of the cosine $m = 0, 1, 2$ and sine $m = 1$ modes.

Each camera aperture was fully constrained for maximal throughput while preserving resolution. The rectangular pinhole size simultaneously limited the chord views to the center stack while also minimizing chord overlap in the same array. The known étendue and responsitivity provides absolute measure of expected current for each diode for a known plasma emissivity profile. The height of NSTX-U vessel required a smaller aperture on the third vertical viewing array to preserve resolution for the smaller fan-beam.

III. SYNTHETIC DIAGNOSTIC

Model total photon emissivities were generated to scope necessary transimpedance gains while also testing the efficacy of tomographic schemes. The emissivities were calculated using known cooling rates coupled with experimental impurity and electron temperature and density radial profiles.[2] The profiles are based off of previous experimental NSTX data placed within the NSTX-U vessel geometry with a P_{rad} of 0.5 MW, consisting mainly of C and Fe emission. The radiated power was mapped poloidally utilizing a plasma equilibrium (generated using the EFIT code[3]) for two cases. The first model including a rotation-induced asymmetry and the second a stationary control.

The two model emissivities were converted into measured brightness profiles through the camera geometry. Two methods were utilized for generating the brightness in order to validate the pinhole optimization. The first method integrated the principal beam through emissivity distribution. The second subdivided the pinhole and diode into sub-surfaces and connected a chord from every sub-pinhole to every sub-diode. Over 10000 chords per diode were traced through the plasma, providing a measure of finite-aperture effects on the brightness. Each of the finite-étendue beams were integrated through the radiated power and totalled. This provided a more accurate representation of the emission, especially as each chord intercepts the conic surfaces of the NSTX-U vessel.

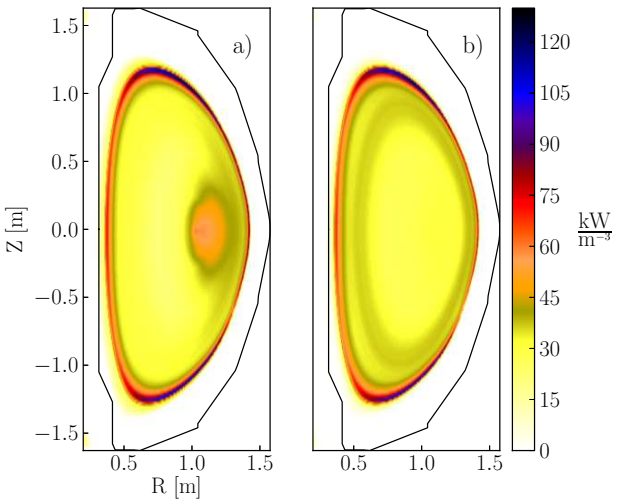

FIG. 2. Model emissivities with (a) and without (b) asymmetry due to rotation (shot 138767).

Results showed that the finite-aperture effects caused a less than 2% variation from the ideal principal beam representation of the chord. In cases where there is substantial gradients in emission perpendicular to the principal ray, the differences were substantially larger. This was mainly seen in chords viewing near the edge of the

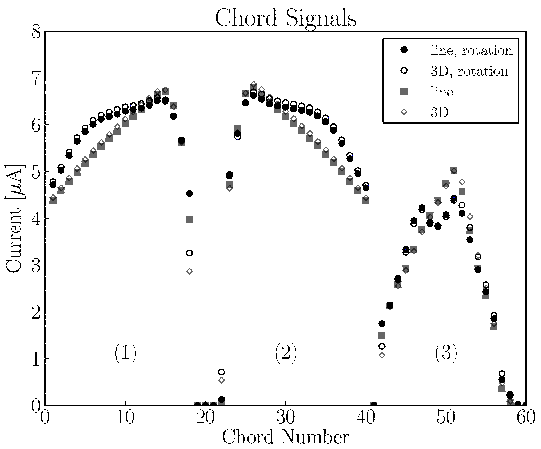

FIG. 3. Expected diode currents on the three cameras for the two model emissivites generated with and without finite-aperture effects

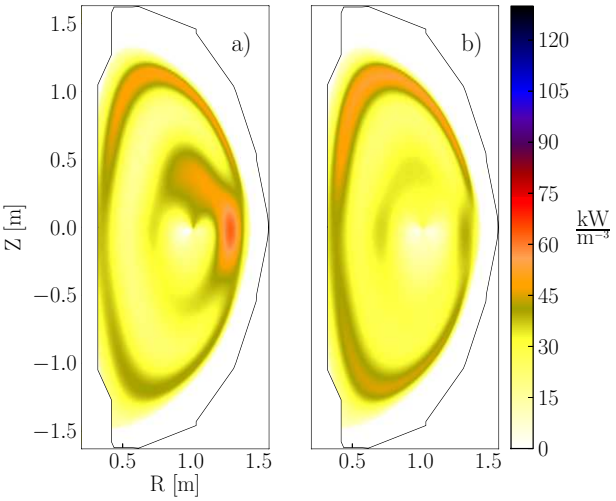

FIG. 4. Flux-Fourier tomographic reconstructions with rotation (a) and without rotation (b)

plasma, understating the necessity of measuring the edge plasma accurately for bolometry. The importance of fine radial resolution is shown fundamentally in the capability for the inversion routines in recovering the dominant and radially-thin edge emission zone.

IV. TOMOGRAPHIC RECONSTRUCTION

The finite-aperture generated brightnesses were used to test tomographic reconstruction of the total radiated power. Representations of the chord integration were parametrized into sets of polar and polar-like basis functions[4,5]. First, the emissivity was assumed to be a function of magnetic flux (using EFIT[3]) with flux-surface variation decomposed by an angular Fourier decomposition. While soft X-ray core emission is not flux dependent[6], significant edge emission is expected to follow the flux expansion typical of the edge plasma. Secondly, Bessel-Fourier polar tomography[5,7,8] was used to test its efficacy for flux-independent reconstruction.

The matrix for inversion was assembled by iterating the principal beam of each chord through the vessel and finding the square-root magnetic flux ($\sqrt{\Psi}$) value at each position. The length of the step size was added fractionally to the nearest $\sqrt{\Psi}$ points where the emission was to be determined. Angular harmonic dependencies followed a similar procedure but were also multiplied by the value of the harmonic at the flux-mapped point. The ill-posed matrix was sensitive to high-spatial frequency variation in $\sqrt{\Psi}$ necessitating the use of second-order Tikhonov regularization[9]. This was done as inversions using singular value decomposition (SVD) could not be used to generate physically relevant solutions. For Bessel-Fourier reconstruction, the parameters of the matrix were calculated by a modified form of equation (9) in [10]

$$f_{ml}(p) = (J_{m+1}(x_{ml}) - J_{m-1}(x_{ml}))\cdot \int_0^{\cos^{-1} p} \cos(m\theta)\sin(x_{ml}(\cos\theta - p))d\theta \quad (1)$$

Additional zero-brightness chords were created at minimum p which existed outside the vessel and distributed equally in angle. This was done to improve the angular validity of the tomographic reconstruction.

The flux-Fourier method could only qualitatively reproduce the significant edge radiated power and rotation induced asymmetry. However, quantitative agreement was found for the flat core emission. Bessel-Fourier reconstructions were distorted by the dominant the edge emission. In principle the elongation of the radiated power can determined using 3 cameras, but the structure of the edge emission is composed of higher Fourier harmonics. Bessel-Fourier tomography is poorly suited for reconstruction in this case due to significant edge emission and plasma shaping.

V. CONCLUSIONS

A design study for a bolometric 2-dimensional poloidal tomography system for NSTX-U was completed. The three AXUV-based pinhole cameras were optimally placed to tomographically reconstruct the total radiated power profile on a model equilibrium. A 3-dimensional camera model was used to minimize finite-aperture effects and determine expected diode signals.

Flux-Fourier and Bessel-Fourier methods were used to recreate model radiated power profiles. It was found that the significant edge emission prevented the use of Bessel-Fourier methods to properly model the emissivity. Flux-Fourier tomography could resolve the edge emission and core asymmetry, but was limited in radial resolution.

This work was performed under US DOE contracts DE-FC02-99ER54512 at MIT and DE-AC02-09CH11466 at PPPL.

[1] R. L. Boivin, J. A. Goetz, E. S. Marmar, J. E. Rice, and J. L. Terry, Review of Scientific Instruments **70**, 260 (1999).
[2] L. Delgado-Aparicio et al., Review of Scientific Instruments (2014), these proceedings.
[3] L. Lao, H. S. John, R. Stambaugh, A. Kellman, and W. Pfeiffer, Nuclear Fusion **25**, 1611 (1985).
[4] G. Fuchs, Y. Miura, and M. Mori, Plasma Physics and Controlled Fusion **36**, 307 (1994).
[5] Y. Nagayama, Journal of Applied Physics **62**, 2702 (1987).
[6] M. C. Borrs and R. S. Granetz, Plasma Physics and Controlled Fusion **38**, 289 (1996).
[7] C. Janicki, R. Décoste, and C. Simm, Phys. Rev. Lett. **62**, 3038 (1989).
[8] R. Granetz and P. Smeulders, Nuclear Fusion **28**, 457 (1988).
[9] Y. Liu, N. Tamura, B. J. Peterson, N. Iwama, and L. E. Group, Review of Scientific Instruments **77**, (2006).
[10] L. Wang and R. S. Granetz, Review of Scientific Instruments **62**, 842 (1991).